Hydrology and
Earth System
Sciences

Open Access

Discussions

EGU

1 **Towards a tracer-based conceptualization of meltwater dynamics**

2 **and streamflow response in a glacierized catchment**

3

4 Running title: Meltwater dynamics and streamflow response

5

6 Daniele Penna[1], Michael Engel[2], Giacomo Bertoldi[3], Francesco Comiti[2]

7

8 [1]Department of Agricultural, Food and Forestry Systems, University of Florence, via San Bonaventura 13, 50145

9 Florence-Firenze, Italy.

10 [2]Faculty of Science and Technology, Free University of Bozen-Bolzano, Piazza dell' Università 5, 39100, Bozen-

11 Bolzano, Italy.

12 [3]Institute for Alpine Environment, European Academy-EURAC, viale Druso 1, 39100, Bozen-Bolzano, Italy

13

14 *Correspondence to*: Daniele Penna (daniele.penna@unifi.it)

15

16 **Abstract**

17 Multiple water sources and the physiographic heterogeneity of glacierized catchments hamper a complete

18 conceptualization of runoff response to meltwater dynamics. In this study, we used environmental tracers (stable

19 isotopes of water and electrical conductivity) to obtain new insight into the hydrology of glacierized catchments, using

20 the Saldur River catchment, Italian Alps, as a pilot site. We analysed the controls on the spatial and temporal patterns of

21 the tracer signature in the main stream, its selected tributaries, shallow groundwater, snowmelt and glacier melt over a

22 three-year period. We found that stream water electrical conductivity and isotopic composition showed consistent

23 patterns in snowmelt-dominated periods whereas the streamflow contribution of glacier melt altered the correlations

24 between the two tracers. By applying two- and three-component mixing models we quantified the seasonally-variable

25 proportion of groundwater, snowmelt and glacier melt at different locations along the stream. We provided four model

26 scenarios based on different tracer signature of the end-members: the highest contributions of snowmelt to streamflow

27 occurred in late spring-early summer and ranged between 70 % and 79 %, according to different scenarios, whereas the

28 largest inputs by glacier melt were observed in mid-summer, and ranged between 57 % and 69 %. In addition to the

29 identification of the main sources of uncertainty, we demonstrated how a careful sampling design is critical in order to

30 avoid underestimation of the meltwater component in streamflow. These results supported the development of a

31 conceptual model of streamflow response to meltwater dynamics in the Saldur catchment likely valid for other

32 glacierized catchments worldwide.

33

34 *Keywords:* snowmelt; glacier melt; groundwater; stable isotopes of water; electrical conductivity; glacierized

35 catchment.

36

37 **1. Introduction**

38   Glacierized catchments are highly dynamic systems characterized by large complexity and heterogeneity due to the

39   interplay of several geomorphic, ecological, climatic and hydrological processes. Particularly, the hydrology of

40   glacierized catchments significantly impacts downstream settlements, ecosystems and larger catchments that are

41   directly dependent on water deriving from snowmelt, glacier melt or high-elevation springs (Finger et al., 2013;

42   Engelhardt et al., 2014). Water seasonally melting from snowpack and glacier bodies can constitute a larger

43   contribution to annual streamflow than rain (Cable et al., 2011; Jost et al., 2012), and is widely used, especially in

44   Alpine valleys, for irrigation and hydropower production (Schaefli et al., 2007; Beniston, 2012). It is therefore pivotal

45   for an effective adoption of water resources strategies to understand the origin of water and to quantify the proportion of

46   snowmelt and glacier melt in streamflow (Finger et al., 2013; Fan et al., 2015). To achieve this goal it is critical to gain

47   a more detailed understanding of the hydrological functioning of glacierized catchments through the analysis of the

48   spatial and temporal variability of water sources and the spatial and seasonal meltwater (snowmelt plus glacier melt)

49   dynamics.

50

51   Hydrochemical tracers (e.g., stable isotopes of water, major ions, electrical conductivity (EC)) are among the most

52   commonly employed tools to characterize hydrological dynamics in glacierized catchments (see Baraer et al. (2015) and

53   references therein). In high-elevation catchments, the temporary storage of winter-early spring precipitation in

54   snowpack and in the glacier body and their melting during the late spring and summer controls the variability in solute

55   and isotopic compositions of stream water (Kendall and McDonnell, 1998). Therefore, hydrochemical tracers allow for

56   an effective identification of water sources and their variability within the catchments and over different seasons,

57   providing essential information about water partitioning and water dynamics and improving our understanding of

58   complex hydrology and hydroclimatology of the catchment, especially in remote regions (Rock and Mayer, 2007; Fan

59   et al., 2015; Xing et al., 2015). Particularly, a few works relied on stable isotopes of water (^{2}H and δ^{18}O) used in

60   combination with EC to evaluate the role played by meltwater in the hydrology of glacierized catchments. For instance,

61   some of these investigations allowed for the separation of streamflow into subglacial, englacial, melt and rainfall-

62   derived components in the South Cascade Glacier, USA (Vaughn and Fountain, 2005), into components due to

63   monsoon rainfall runoff, post-monsoon interflow, winter snowmelt and groundwater glacier melt (the latter estimated

64   up to 40 % during summer and monsoon periods) in the Ganga River, Himalaya (Maurya et al., 2011), and into

65   snowmelt, ice melt and shallow groundwater components in Arctic catchments characterized by a gradient of

66   glacierization (Blaen et al., 2014). Other researchers assessed the possibility to use isotopes and EC as complementary

67   tracers, in addition to water temperature, to identify a permafrost-related component in spring water in a glacierized

68   catchment in the Ortles-Cevedale massif, Italian Alps (Carturan et al., in press). Finally, two recent studies used stable

69   isotopes and EC over a three-year period to assess water origin and streamflow contributors in the Saldur River

70   catchment, Italian Alps. Penna et al. (2014) showed a preliminary analysis on the highly complex EC and isotopic

71   signature of different waters samples in the catchment, identifying, however, distinct tracer signals in snowmelt and

72   glacier melt. These two end-members dominated the streamflow throughout the late spring and summer, whereas liquid

73   precipitation played a secondary role, limited to rare intense rainfall events. They also assessed, without quantifying it,

74   the switch from snowmelt- to glacier melt-dominated periods, and estimated that the snowmelt fraction in groundwater

75   ranged between 21 % and 93 %. Engel et al. (2016) employed two- and three-component mixing models to quantify the

76   relative contribution of snowmelt, glacier melt and groundwater to streamflow during seven representative melt-induced

77   runoff events sampled at high frequency at two cross-sections of the Saldur River. They observed marked reaction of

78   tracers and streamflow both to melt and rainfall inputs, identifying hysteretic loops of contrasting directions. They

Hydrology and
Earth System
Sciences
Discussions
Open Access
EGU

79   estimated the maximum contribution of snowmelt during June and July events (up to 33 %) and of glacier melt during

80   the August events (up to 65 %). However, a quantification of the variations of streamflow components not only at the

81   seasonal scale but also at different spatial scales across the catchment was not performed and a conceptual model of

82   meltwater dynamics not presented. Therefore, despite the number of studies that have conducted hydrological tracer-

83   based investigations in high-elevation mountain catchments, there is still the need to gain a better comprehension of the

84   factors determining the complex hydrochemical signature of stream water and groundwater in glacierized catchments.

85   This research builds on the existing database for the Saldur River and on the first results presented in Penna et al. (2014)

86   and Engel et al. (2016) to improve the knowledge on the complex hydrology and the water sources dynamics in

87   glacierized catchments. Specifically, we aim to:

88   - assess the controls on the spatial and temporal variability of the isotopic composition and EC in the main stream,

89   tributaries and springs in the Saldur River catchment;

90   - analyse the relation between the tracer signature and streamflow variability;

91   - quantify the proportion of snowmelt and glacier melt in streamflow at different stream locations and at different times

92   of the year, as well as the related uncertainty;

93   - derive a conceptual model of streamflow response to meltwater dynamics.

94

95   **2. Study area**

96   The research has been conducted in the upper portion of the Saldur/Saldura River catchment, Vinschgau/Venosta

97   Valley, Eastern Italian Alps (Fig. 1). The catchment size is 61.7 km^2 and altitude ranges between 1632 m a.s.l. at the

98   outlet (46°42'42.37"N, 10°38'51.41"E) and 3725 m a.s.l.. A glacier lies in the upper part of the catchment, with an

99   extension of 2.28 km^2 in 2013 (Galos and Kaser, 2014). The glacier lost 21 % of its area from 2005 to 2013 (Galos,

100   2013). Several glacier-fed and non-glacier-fed lateral tributaries contribute to the Saldur River streamflow, and various

101   springs, apparently connected or not connected to the main stream, can be found on the valley floor and at the toe of the

102   hillslopes in the mid-upper part of the catchment. Rocks are metamorphic, mainly gneisses, mica-gneisses and schists.

103   Land cover changes with elevation typically varying from Alpine forests (up to about 2200 m a.s.l.) to shrubs to Alpine

104   grassland, bare soil and rocks above 2700 m a.s.l.. The area is characterized by a continental climate with average

105   annual air temperature of 6.6 °C and precipitation as low as 569 mm/yr (at 1570 m a.s.l.), likely increasing up to 800-

106   1000 mm/yr in the upper parts of the catchment. At 3000 m a.s.l., the total precipitation can be estimated, using the

107   approach of Mair et al. (2015), to be about 1500 mm, 80% of which falls as snow. The hydrological regime is typically

108   nivo-glacial with minimum streamflow recorded in winter and high flows occurring from late spring to mid-summer,

109   when marked diurnal streamflow cycles occur, related to snow- and glacier melt (Mutzner et al., 2015). More detailed

110   information on the study area are reported in Mao et al. (2014) and Penna et al. (2014).

111

112   **3. Materials and methods**

113   **3.1 Hydrological and meteorological measurements**

114   Field measurements were conducted from April 2011 to October 2013. Meteorological data were recorded at 15-min

115   temporal resolution by two stations located at 2332 m a.s.l. and 1998 m a.s.l. (Fig. 1a). Stage in the Saldur River was

116   recorded every 10 minutes by pressure transducers at the catchment outlet and at two river sections labelled Lower

117   Stream Gauge (S3-LSG, 2150 m a.s.l.) and Upper Stream Gauge (S5-USG, 2340 m a.s.l.), that defined two nested

118   subcatchments with an area of 18.6 km^2 and 11.2 km^2 (Fig. 1a). Streamflow values were obtained by 82 discharge

119   measurements acquire by the salt dilution method during various hydrometric conditions over the three study years.

120 Water level was also continuously measured on a left tributary (T2-SG, 2027 m a.s.l., Fig. 1b) draining an area of 1.7

121 km^2 but a robust rating curve was not available to derive streamflow.

122

3.2 Tracer sampling and measurement

124 Samples used in this study and analysed for the two tracers were collected from snowmelt, glacier melt, stream water

125 and groundwater. Snowmelt was sampled in late spring-early summer collecting water dripping from the residual

126 snowpack at different elevations and different locations. Snowmelt was sampled on three occasions in summer 2012

127 (end of June, beginning and end of July), at elevations roughly between 2150 m a.s.l. and 2350 m a.s.l., and on nine

128 occasions in summer 2013 (June, July and August) at elevations roughly between 2150 m a.s.l. and 2600 m a.s.l..

129 Glacier melt was sampled from small rivulets flowing on the glacier surface, roughly at 2800 m a.s.l. in July and August

130 2012, and in July, August and September 2013. Grab stream water samples were taken approximately monthly at eight

131 locations in the Saldur River (labelled from S1 to S8), at elevations spanning from 1809 m a.s.l. (S1) and 2415 m a.s.l.

132 (S8), and from five tributaries (labelled from T1 to T5), at elevations between 1775 m a.s.l. (T1) and 2415 m a.s.l. (T5,

133 Fig. 1b). Samples at T1 were taken only in 2012, and samples at T3 only in 2011. In 2013 samples were collected

134 monthly during clear days only from the river at four sections (S1, S3-LSG, S5-LSG, S8), respecting the same time of

135 the day on each occasion in order to ensure consistency and comparability between measurements. The

136 representativeness of these samples for the typical melting conditions in the catchment was visually ensured by

137 comparing the hydrographs of the sampled days with the ones of the corresponding months during the three monitored

138 years. No wells are available in the study catchment, thus spring water was assumed to represent shallow groundwater

139 (Kong and Pang, 2012; Racoviteanu et al., 2013). Four springs (labelled from SPR1 to SPR4) localized near the outlet

140 of USG, between 2334 m a.s.l. and 2360 m a.s.l. were sampled monthly during the three study years. On one occasion

141 (17 October 2011), no sample was taken from SPR1 because it was found dry. Additionally, monthly samples were also

142 taken from June to September 2013 from two springs on the left valley hillslope, SPR6 and SPR7, at 2512 m a.s.l. and

143 2336 m a.s.l., respectively (Fig. 1b). A list of all sampling locations with their main characteristics is reported in Penna

144 et al. (2014).

145 In addition to the monthly sampling, stream water samples were collected at USG and LSG during seven runoff events

146 induced by meltwater in July and August 2011, and June, July and August 2012 and 2013. Samples were collected from

147 10:00 of one day to 10:00 (or longer) on the following day at hourly frequency during the day, until 22:00, and every

148 three hours during the night. For those events, two- and three-component mixing models were applied to quantify the

149 fraction of snowmelt and glacier melt in streamflow. Description of the runoff events and hydrograph separation results

150 are reported in Engel et al. (2016). The number of samples collected from the different water sources at the various

151 locations and years used in this study is reported in Table 1.

152

153 EC was determined directly in the field by means of a conductivity meter with a precision of ± 0.1 µS/cm. The EC

154 meter was routinely calibrated to ensure consistency among the measurements.

155 Grab water samples for isotopic determination were taken by 50 mL HDPE bottles with two caps and completely filled

156 to avoid head space. Isotopic analysis was carried out by an off-axis integrated cavity output spectroscope tested for

157 precision, accuracy and memory effect in previous intercomparison studies (Penna et al., 2010; 2012). The observed

158 instrumental precision, considered as the long-term average standard deviation, is 0.5 ‰ for δ^{2}H and 0.08 ‰ for δ^{18}O.

159 Isotopic values are presented using the δ notation referred to the SMOW2-SLAP2 scale provided by the International

160 Atomic Energy Agency.

161

162 **3.3 Two- and three-component mixing models and underlying assumptions**

163 A one-tracer, two-component mixing model (Pinder and Jones, 1969; Sklash and Farvolden, 1979) was used to quantify

164 and separate two streamflow components (groundwater and snowmelt), and a two-tracer, three-component mixing

165 model (Ogunkoya and Jenkins, 1993) was used for three streamflow components (groundwater, snowmelt and glacier

166 melt. Mixing models were applied only to 2013 data because in that year water samples were collected at four locations

167 along the main stream (S1, S3-LSG, S5-USG and S8) at the same time of the day on all sampling occasions. This was

168 critical to ensure comparability of the results, given the high diurnal variability of streamflow and associated isotopic

169 composition and EC, especially during the summer.

170

171 The following simplifying assumptions were made for the application of the mixing models:

172 - Streamflow at each selected sampling location of the Saldur River was a mixture of two components, viz. groundwater

173 and snowmelt, or three components, viz. groundwater, snowmelt and glacier melt. The influence of precipitation was

174 considered negligible because samples were collected during non-rainy periods, and particularly during warm, clear

175 days when the meltwater input to runoff was remarkable and overwhelmed the possible presence of rain water in

176 streamflow.

177 - The highest contribution of snowmelt to streamflow was assumed deriving from snow melting at an approximate

178 elevation of 2800 m a.s.l.. The elevation band between 2800 m a.s.l. and 2850 m a.s.l. was the one with the largest area

179 in the catchment ($3.4 \ km^2$), where much snow can accumulate, as confirmed by the analysis of snow cover data from

180 Moderate-resolution Imaging Spectroradiometer (MODIS) images (c.f. Engel et al., 2016).

181

182 The three-component mixing model was based on isotopic and EC data (Maurya et al., 2011; Penna et al., 2015) and

183 first applied to all samples collected in the Saldur River in 2013. When the three-component mixing model yielded

184 inconsistent results, typically in May and June and partially in October, it was inferred that there was no glacier melt

185 component in streamflow, thus the two-component mixing model was performed to separate the snowmelt from the

186 groundwater component. As a preliminary step, both EC and isotopes were used in the two-component mixing model.

187 The resulting estimates were strongly correlated ($p < 0.01$) but, overall, snowmelt fractions computed for May and June

188 using isotopes were smaller compared to those computed through EC. In agreement with our previous work in the

189 Saldur catchment (Engel et al., 2016), we decided to present EC-based results for the sampling days in May and June

190 because of the large difference between the low EC of the snowmelt end-member and the relatively high EC of the

191 stream that provided lower uncertainties in the estimated fractions compared to isotopes (Genereux et al., 1998).

192 Conversely, for the sampling day in October, there was a relatively small difference between the EC of the groundwater

193 end-member and the EC of the stream, while the difference in the isotopic signal of the end-members was greater, and

194 thus the uncertainty in the estimated fractions was lower. Therefore, in these cases we used isotopes instead of EC in the

195 two-component mixing model.

196

197 Based on the stated assumptions, the following mass balance equations can be written for periods when only snowmelt

198 and groundwater contributed to streamflow:

199 $SF = SM + GW$ (Eq. 1)

200 $1 = sm + gw$ (Eq. 2)

201 $\delta_{SF} = sm \cdot \delta_{SM} + gw \cdot \delta_{GW}$ (Eq. 3)

202 and

203 $EC_{SF} = sm \cdot EC_{SM} + gw \cdot EC_{GW}$ (Eq. 4)

204 where SM, GW, and SF denote snowmelt, groundwater and streamflow, respectively; sm and gw indicate the

205 streamflow fraction due to snowmelt and groundwater, respectively; and the notation δ and EC are used for the isotopic

206 composition and the EC of each component, respectively. Eqs. 1-4 can be solved for the unknown sm as follows:

207 $sm(\%) = \frac{\delta_{SF} - \delta_{GW}}{\delta_{SM} - \delta_{GW}} \cdot 100$ (Eq. 5)

208 or, using EC:

209 $sm(\%) = \frac{EC_{SF} - EC_{GW}}{EC_{SM} - EC_{GW}} \cdot 100$ (Eq. 6)

210 The gw component can be then calculated by Eq. 2. Analogously, the following mass balance equations can be written

211 for periods when snowmelt, glacier melt and groundwater contributed to streamflow:

212 $SF = SM + GM + GW$ (Eq. 7)

213 $1 = sm + gm + gw$ (Eq. 8)

214 $\delta_{SF} = sm \cdot \delta_{SM} + gm \cdot \delta_{GM} + gw \cdot \delta_{GW}$ (Eq. 9)

215 $EC_{SF} = sm \cdot EC_{SM} + gm \cdot EC_{GM} + gw \cdot EC_{GW}$ (Eq. 10)

216 where, in additions to symbols used in Eqs. 1-6, GM denotes glacier melt, and gm indicates the streamflow fraction due

217 to glacier melt. Eqs. 7-10 can be solved for the unknown sm and gm as follows:

218 $sm\ (\%) = \frac{(\delta_{SF} - \delta_{GW}) \cdot (EC_{GM} - EC_{GW}) - (\delta_{GM} - \delta_{GW}) \cdot (EC_{SF} - EC_{GW})}{(\delta_{SM} - \delta_{GW}) \cdot (EC_{GM} - EC_{GW}) - (\delta_{GM} - \delta_{GW}) \cdot (EC_{SM} - EC_{GW})} \cdot 100$ (Eq. 11)

219 $gm\ (\%) = \frac{(\delta_{SF} - \delta_{GW}) \cdot (EC_{SM} - EC_{GW}) - (\delta_{SM} - \delta_{GW}) \cdot (EC_{SF} - EC_{GW})}{(\delta_{GM} - \delta_{GW}) \cdot (EC_{SM} - EC_{GW}) - (\delta_{SM} - \delta_{GW}) \cdot (EC_{GM} - EC_{GW})} \cdot 100$ (Eq. 12)

220 The gw component can be then calculated by Eq. 8.

221

222 The uncertainty of the end-member fractions calculated through the two-component mixing model was quantified

223 following the method of Genereux (1998) at the 70 % confidence level. The uncertainty of the end-member fractions

224 calculated through the three-component mixing model was determined by varying the isotopic composition and EC of

225 each end-member by ± 1 standard deviation (Carey and Quinton, 2005; Engel et al., 2016). All mixing models were

226 applied using both δ^2H and $\delta^{18}O$ data; however, results based on $\delta^{18}O$ measurements showed a greater uncertainty than

227 the those derived by δ^2H data due to the instrumental performance (Penna et al., 2010). Thus, all results related to

228 isotopes reported in this study are based on δ^2H data.

229

230 **3.4. Scenarios of mixing model application**

231 The spatial and temporal variability in end-member tracer signal is usually very difficult to characterise at the

232 catchment-scale (Hoeg et al., 2000), especially in glacierized catchments (Jeelani et al., 2016) and has a critical impact

233 on the application of mixing models. In order to take such variability and its associated uncertainty into account, we

234 identified four different scenarios considering the groundwater end-member based on springs or stream during baseflow

235 conditions, and time-invariant or monthly-variable isotopic composition and EC of the snowmelt end-member (Table

236 2). Particularly, in scenarios A and C, the groundwater end-member was based on the average isotopic composition and

237 EC of samples taken from springs during baseflow conditions in fall (springs were not sampled during winter due to

238 limited accessibility of the area), consistently with Engel et al. (2016) (Table 3). In scenarios B and D, the groundwater

239 end-member was defined as the average of the tracer signal of different stream samples taken during baseflow

240 conditions (late fall and winter of the three study years), at the four Saldur River locations selected in 2013 (Table 3).

241 For the definition of these two groundwater end-members, we selected the samples taken during baseflow conditions

242 when we assumed that there was no or negligible contribution of snowmelt, glacier melt and rainfall to streamflow. It is

243 important to note that we consider as groundwater component both the spring baseflow and the stream baseflow,

244 because the hydrochemistry of streams during baseflow conditions generally integrates and reflects the hydrochemistry

245 of the (shallow) groundwater at the catchment scale (Skash, 1990; Klaus and McDonnell, 2013; Fischer et al., 2016).

246

247 In scenarios A and B the tracer signature of the snowmelt end-member was considered time-invariant (Maurya et al.,

248 2011) (Table 4). Following Engel et al. (2016), the high-elevation (2800 m a.s.l.,) snowmelt isotopic composition was

249 identified through the regression analysis of snowmelt samples collected at different elevations in June 2013, according

250 to Eq. 13 (R^2 = 0.616, n = 7, p < 0.05):

251 $\delta^2H\ (‰) = -0.0705 \cdot elevation\ (m\ a.s.l.) + 37.261$ (Eq. 13)

252 EC_{SM} was based on the average EC of all snowmelt samples collected in 2013, without applying any regression-based

253 modification.

254 In scenarios C and D, the isotopic composition of high-elevation snowmelt end-member was considered seasonally-

255 variable, to take into account that water from melting snowpack typically undergoes progressive fractionation and isotopic

256 enrichment over the season (Taylor et al., 2001; Lee et al., 2010) (c.f. Section 4.1). A depletion rate of -7.0 ‰ in δ^2H for

257 100 m of elevation rise was derived from Eq. 13, and used to estimate the isotopic composition of high-elevation snowmelt

258 from snowmelt samples collected monthly at different elevations from May to August 2013 (Table 4). Analogously, the

259 average EC of snowmelt samples taken monthly was adopted.

260 For all scenarios, the isotopic signature and EC of the glacier melt end-member was considered monthly-variable (Table

261 5 and Section 4.1).

262

263 **4. Results**

264 **4.1 Isotopic composition and EC of the different water sources**

265 Snowmelt sampled from snow patches in summer 2012 and 2013 ranged in δ^2H from -106.1 ‰ to -139.5 ‰ and in EC

266 from 3.2 µS/cm and 77.0 µS/cm. Glacier melt displayed a marked enrichment in heavy isotopes over summer,

267 particularly in 2013 (Table 5). The spatial variability in the isotopic composition of glacier melt was generally small,

268 with spatial standard deviations ranging between 1.3 ‰ and 6.5 ‰. The EC of glacier melt was very low and little

269 variable in space and in time (average: 2.1 µS/cm, standard deviation: 0.7 µS/cm, n = 16) for 2012 and 2013 overall,

270 even though a slight progressive increase in EC was observed in 2013 (Table 5).

271

272 The Saldur catchment was characterized by a marked variability of tracer signature within the same water compartment

273 (i.e., main stream water, tributary water, groundwater) both in time and in space (Table 6, Fig. 2 and 3). There was a

274 statistically significant difference in δ^2H and EC between the Saldur River and its sampled tributaries for the entire

275 sampling period (Mann-Whitney test with p=0.004 and p<0.001, respectively). On average, stream water showed more

276 isotopically negative and variable values and had lower EC and higher variability in the summer than in fall and winter.

277 Moreover, the main stream had more depleted isotopic composition and lower EC compared to the tributaries (Table 6).

278 Spring water was the most enriched water source during the fall but became more depleted compared to stream water

279 during the summer when it also showed higher EC. The coefficient of variations of δ^2H for groundwater were generally

280 slightly higher than for the stream water in all seasons, but the variability in EC was similar to that of the Saldur River

281 and smaller than that of the tributaries (Table 6).

7

Hydrology and
Earth System
Sciences
Discussions

Open Access

EGU

282

283   Overall, the median isotopic composition of stream water in the Saldur River varied slightly, but long error bars indicate

284   a great temporal variability (Fig. 2). On the contrary, tributaries showed a wider range in the isotopic composition but a

285   smaller temporal variability compared to the main stream (Fig. 2a). EC showed an increasing trend from upper to lower

286   locations along the Saldur River (although with a slight interruption at S3-LSG) (Fig. 2b). On average, tributaries had

287   higher EC compared to all other waters sampled in the catchment. Interestingly, T4 was the stream location with the

288   most negative isotopic composition and highest EC. Groundwater tracer signature was overall intermediate between the

289   main stream and the tributaries with a remarkable difference between SPR1-3 and SPR4.

290   Despite the strong variability, some spatial and temporal patterns can be observed (Fig. 3). For instance, all locations in

291   June and early July 2012 showed isotopically depleted water and so did, overall, locations T4 and T5. Groundwater in

292   SPR4 was constantly more enriched than the other springs (Fig. 3a). The increasing trend in EC from the highest Saldur

293   River location (S8) down to the lowest location (S1) in July and August of both years is also clearly visible, as well as

294   the temporally constant and relatively very high EC of tributary water at T4 and very low EC of groundwater in SPR4

295   (Fig. 3b).

296

297   The mixing-plot between δ^2H and EC of stream water and groundwater of all sampling locations further highlights the

298   differences in the tracer signature of the main stream, the tributaries and the springs (Fig. 4). Overall, the main stream

299   showed a wider range in isotopic composition compared to the tributaries, in agreement with the long error bars of

300   locations S1-S8 in Fig. 2. EC of the Saldur River was also more variable than EC in the other waters, except for T5 that

301   plots separately compared to other tributaries and the main stream. The spring data points only partially overlap with the

302   main stream data points: indeed, the tracer signal of the main stream water is upper-bounded by springs SPR1-3 and,

303   partially by T2-SG, and laterally, towards the less negative isotopic values, by SPR4. Only the tracer signal of T1, a left

304   tributary flowing into the Saldur River a few hundred meters downstream S1, lies within the main stream data, but

305   samples were taken only in 2012 and so a robust comparison could not be performed.

306

307   **4.2 Relation between the two tracers, streamflow and meltwater fractions**

308   The relation between δ^2H and EC of stream water samples collected at S5-USG and S3-LSG on the same days in 2011,

309   2012 and 2013, and averaged by month, shows different behaviours according to the sampling period (Fig. 5). Overall,

310   sampling days in May, June and September were characterized by lower mean daily temperatures and stream discharge,

311   much higher EC and more depleted isotopic composition compared to sampling days in July and August (Table 7). The

312   relation between the two tracers is statistically significant in the colder months whereas it is more scattered and not

313   statistically significant during the warmest months (Fig. 5). The range of δ^2H values was slightly larger in the mid-

314   summer period compared to May, June and September (16.7 ‰ vs. 15.1 ‰); on the contrary, the range of EC values

315   was much larger in the spring-late summer period compared to July and August (173.9 µS/cm vs. 77.1 µS/cm).

316

317   Streamflow during the summer melt runoff events sampled hourly at the two monitored cross sections S5-USG and S3-

318   LSG is positively correlated with the fraction of meltwater (snowmelt plus glacier melt components) (Fig. 6).

319   Streamflow is presented for comparison purposes both in terms of specific discharge and relative to bankfull discharge,

320   the latter estimated in the two reaches based on direct observations during high flows. A closer inspection of the figure

321   reveals the occurrence of hysteretic loops between streamflow and meltwater at both locations more clearly evident for

322   events on 12-13 July 2011, 10-11 August 2011 and 21-22 August 2013 at S5-USG, due to their magnitude.

Hydrology and
Earth System
Sciences
Discussions

323 Nevertheless, a general positive trend between the two variables is observable, with meltwater fractions increasing

324 when streamflow increased ($R^2 = 0.48$, n = 130; p < 0.01 at S5-USG; $R^2 = 0.26$, n = 114; p < 0.01 at S3-LSG). The

325 relation between meltwater fractions (computed as average of the results of the four mixing model scenarios, see

326 Section 4.4) and streamflow is also plotted for the samples taken monthly in 2013, indicated by the stars in Fig. 6. The

327 samples collected during the 2013 campaigns plot consistently with the samples taken during the melt runoff events at

328 both locations, overall agreeing with the positive trend of the meltwater-streamflow relation (Fig. 6).

329

330 **4.3 Quantification of snowmelt and glacier melt in streamflow and associated uncertainty**

331 The results of the two- and three-component mixing models reveal a seasonally-variable influence of snowmelt and

332 glacier melt on streamflow, with estimated fractions generally decreasing from the highest to the lowest location (Fig.

333 7). Overall, the proportion of snowmelt in stream water was comparable for the four sampling days in August,

334 September and October. Estimated snowmelt fractions were highest on 19 June, up to 79 ± 6 % (scenario B) at S8. Field

335 observations and MODIS data (Engel et al., 2016) revealed that the glacier surface was still covered with snow until the

336 end of June. All four mixing model scenarios agree with these observations and estimate no contribution of glacier melt

337 to streamflow on the sampling days in May and June, and only partially on 18 October (Fig. 7). Glacier melt was an

338 important component of streamflow on 16 July, especially according to scenarios A and B, and dominated the

339 streamflow in mid-August according to all scenarios, with peak estimates at S8 ranging from 50 - 66 % (scenario D) to

340 68 - 71 % (scenario A). On 12 August, meltwater was the prevalent streamflow component at the three upper sampling

341 locations and was still relevant at the lowest sampling location.

342

343 Overall, the four scenarios provide similar patterns of meltwater dynamics with higher similarities between scenarios A

344 and B, and between scenarios C and D. Indeed, strong correlations exist between the estimates of the same component

345 computed in each scenario, with R^2 for all possible combinations ranging between 0.91 and 0.997 for groundwater, 0.68

346 and 0.94 for snowmelt, and 0.74 and 0.94 for glacier melt (n = 22, p < 0.01 for all correlations). Despite the general

347 agreement, differences in the estimated streamflow components among to the four scenarios do exist. Particularly,

348 scenarios C and D yield higher overall proportions of snowmelt compared to scenarios A and B, and scenarios A and D

349 provide the overall highest and smallest fraction of glacier melt, respectively. Furthermore, scenarios C and D provide

350 larger proportions of snowmelt and smaller proportions of glacier melt in July compared to the two other scenarios (Fig.

351 7). Overall, the uncertainty associated to the computation of the streamflow fractions is larger for scenarios A and C

352 than for scenarios B and D (error bars in Fig. 7). It is worth mentioning that different proportions of meltwater

353 components at the same stream location could be estimated according to the sampling time of the day. For the melt-

354 induced runoff events sampled at high temporal resolution in 2011, 2012 and 2013, the maximum contribution of

355 meltwater to streamflow occurred at the streamflow peak or within an hour after the streamflow peak in 79 % of the

356 observations, whereas the maximum contribution of meltwater was observed within two hours before the streamflow

357 peak in the remaining 21 % of the cases. Therefore, sampling several hours before or after the streamflow peak can lead

358 to an underestimation of the meltwater fractions in streamflow (Fig. 8). However, the differences in meltwater fractions

359 between samples collected at the streamflow peak and samples collected after the streamflow peak are lower and less

360 variable (shorter error bars) than the ones computed before the streamflow peak (Fig. 8).

361

362 **5. Discussion**

363 **5.1 Controls on the spatio-temporal patterns of the tracer signal**

364   Glacier melt was characterized by similar isotopic composition in 2012 and 2013 and, most of all, by a marked isotopic
365   enrichment and a slight EC increase over the summer season (Table 5). Yde et al. (2016) showed similar trends in the
366   isotopic composition of meltwater draining Mittivakkat Gletscher, Greenland, for two summers, and Zhou et al. (2014)
367   reported an isotopic enrichment in the firnpack during the early melting season on a glacier in the Tibetan Plateau.
368   However, other studies have reported a strong inter-annual variability in the isotopic signature of glacier melt
369   (Yuanqing et al., 2001) or fairly consistent values over time (Cable et al., 2011; Maurya et al., 2011; Ohlanders et al.,
370   2013; Racoviteanu et al., 2013). In our case, since melting of the surface ice determines no isotopic fractionation
371   (Jouzel and Souchez,1982), as confirmed by glacier melt samples falling on the local meteorological water line (Penna
372   et al., 2014), the progressive enrichment could be explained by contributions from deeper portions of the glacier surface
373   with increasing ablation over the melting season or sublimation of surface ice (Stichler et al., 2001). More data from
374   this and other glacierized site should be acquired to better assess this behaviour that we believe must be taken into
375   account in the application of mixing models for the estimation of glacier melt contribution to streamflow in different
376   seasons.
377
378   More negative δ^2H values and lower EC observed in the Saldur River and in its tributaries during the summer than
379   during the winter (Table 6) clearly indicate contributions of meltwater, typically isotopically depleted and diluted in
380   solutes. However, differences exist in the tracer signal among the main stream and the tributaries. The more negative
381   values and the much lower EC of the Saldur River in summer compared to the tributaries (Table 6) suggest important
382   contributions of both depleted snowmelt from high-elevations and almost solute-free glacier melt to the main stream,
383   but less glacier melt contributions to the tributaries. The higher difference for the coefficients of variation between
384   summer and fall-winter in the Saldur River with respect to the tributaries (Table 6) confirms greater inputs of waters
385   with contrasting isotopic signals (depleted snowmelt and more enriched glacier melt) but relatively similar low EC
386   (Maurya et al., 2011). This observation is corroborated by the larger temporal variability (longer error bars) in the
387   isotopic composition of the main stream compared to the tributaries, by the similar temporal variability in EC (Fig. 2),
388   and by the larger span of δ^2H values in the main stream compared to the tributaries visible in the mixing plot (Fig. 4).
389
390   The same isotopic composition of the Saldur River and the springs (Table 6, despite the lack of temporal consistency)
391   and the partially overlap of the spring data points with the stream data points in the mixing plot (Fig. 4) suggest
392   connectivity between the main stream and shallow groundwater, in agreement with observations in other glacierized
393   catchments (Hindshaw et al., 2011; Magnusson et al., 2014). However, a large variability in the tracer signal of springs
394   was observed (Figs. 3-5) highlighting the complex hydrochemistry of the groundwater system (Brown et al., 2006;
395   Hindshaw et al., 2011; Kong and Pang, 2012). The depleted signal in summer months (Table 6) suggests a role of
396   snowmelt in groundwater recharge (Baraer et al., 2015; Fan et al., 2015; Xing et al., 2015). At the same time, the
397   relatively high EC during summer demonstrates solute concentration and suggests longer residence times and/or flow
398   pathways (and thus long contact with the soil particles) of infiltrating meltwater before recharging the groundwater
399   (Brown et al., 2006; Esposito et al., 2016). The similar coefficients of variations of the two tracers in summer and fall
400   indicate less inter-seasonal differences in water inputs to the springs compared to the streams and suggest continuous
401   groundwater recharge even at the end of the melting seasons, pointing out again to relatively long travel times and
402   recharge times.
403

Hydrology and
Earth System
Sciences
Discussions

Open Access

EGU

404   We mainly attribute the large spatial and temporal variability of tracers in stream water and groundwater to the control
405   exerted by climate (seasonality), topography and geological settings. For instance, the depleted waters at all locations in
406   June and early July 2012 (Fig. 3a) indicate heavy snowmelt contributions, consistently with the results of the mixing
407   models (Fig. 7), clearly reflecting a climatic control (snow accumulation during the winter-early spring and subsequent
408   melting). The increasing trend in EC from S8 to S1 during summer periods (Fig. 3b), consistently with other works
409   (Kong and Pang, 2012; Fan et al., 2015), reflects the combined effect of lower elevations, smaller snow-covered area,
410   decreasing glacierized area, progressively decreasing fractions of meltwater and proportional increase of groundwater
411   contributions (Fig. 7), and inflows by groundwater-dominated lateral tributaries.
412   The tracer signal of S3-LSG (Fig. 2) reflected the influence of the tributary T4, upstream of S3-LSG that plotted
413   separately in the mixing diagram (Fig. 4). A combination of depleted isotopic composition (typical of meltwater) and
414   high EC (typical of groundwater) was very rare in the catchment, and we do not have evidences to explain the origin of
415   tributary T4 and the reason of its tracer signature. Analogously, our data did not provide robust explanations about the
416   more enriched isotopic composition and the constantly much lower EC of SPR4 compared to other springs (Figs. 3 and
417   4). Ongoing and future analyses of major anions and cations will help to shed some light on the origin of T4 and SPR4.
418
419   **5.2 Seasonal control on the δ^2H-EC relation and on meltwater fractions**
420   As observed elsewhere (e.g., Hindshaw et al., 2011; Maurya et al., 2011; Blaen et al., 2014), streamflow in the main
421   stream increased during melting periods, EC decreased due to the dilution effect and the isotopic composition generally
422   shifted towards depleted values reflecting the meltwater signal. However, the two tracers were strongly correlated only
423   in May, June and September (Fig. 5), when glacier melt was negligible or absent (Fig. 7) because the tracer signal in the
424   stream reflected the low EC and the depleted isotopic composition of snowmelt. Conversely, during mid-summer, when
425   glacier melt significantly contributed to streamflow (Fig. 7), the relation between the two tracers became weak (Fig. 5),
426   because glacier melt had very low EC but was not as isotopically depleted as snowmelt. Having multiple tracers is of
427   certain usefulness when investigating water sources and mixing processes (Barthold et al., 2011), especially in highly
428   heterogeneous environments (Hindshaw et al., 2011), and is essential for the identification of various streamflow
429   components. However, it is important to know the periods when only one tracer could be reliably used, at least for
430   assessing meltwater inputs, especially in glacierized catchments, where logistical constraints are always challenging.
431
432   The hysteretic behaviour observed between streamflow and meltwater fraction for the melt-induced runoff events (Fig.
433   6) reflects the hysteresis observed in the relation between streamflow and EC, suggesting contributions from water
434   sources characterized by different temporal dynamics (Dzikowski and Jobard, 2012). The combination of highest
435   streamflow and highest meltwater proportion was obtained at both stream sections in June due to the remarkable
436   contribution of meltwater from the relatively deep snowpack in the upper part of the catchment. It is worth to highlight
437   how the meltwater fraction can frequently represent a substantial (> 50 %) proportion of the bankfull discharge, both
438   during snow and glacier melt flows. This implies that future changes in both runoff components will likely have
439   important consequences for the morphological configuration of high-elevation streams like the Saldur River, especially
440   in the wider, braided reaches more responsive to variations in water and sediment fluxes (Wohl, 2010).
441
442   **5.3 Role of snowmelt and glacier melt on streamflow**
443   The spatial and temporal patterns of meltwater dynamics are consistent with those estimated in other high-elevation
444   catchments worldwide. For instance, the dominant role of snowmelt in late spring-early summer and of glacier melt

Hydrology and
Earth System
Sciences
Discussions

Open Access

EGU

445 later in summer was observed across different sites in Asia, North America, South American and Europe (Aizen et al.,

446 1996; Cable et al., 2011; Ohlanders et al., 2013; Blaen et al., 2014, respectively). The decreasing contribution of

447 meltwater from the upper to the lower stream locations from June to October shown almost consistently by all scenarios

448 (Fig. 7) is related to the increasing distance from the glacier and catchment size, and decreasing elevation, in agreement

449 with results from other sites (Cable et al., 2011; Prasch et al., 2012; Racoviteanu et al., 2013; Marshall et al., 2014).

450 Moreover, lateral contributions from non-glacier fed tributaries and/or dominated by groundwater increased the

451 groundwater fraction in streamflow as well and proportionally decreased the meltwater fraction (Marshall et al., 2014;

452 Fan et al., 2015).

453

454 Our estimates of snowmelt contribution to streamflow during the melting season are consistent with those reported in

455 other studies (Carey and Quinton, 2004; Mukhopadhyay and Khan, 2015) and with those found in the same catchment

456 during individual runoff events (Engel et al., 2016). It is more difficult to compare our computed fractions of glacier

457 melt in stream water with estimates in other sites because they can be highly depended on the yearly climatic

458 variability, on the proportion of glacierized area in the catchment and because they are usually reported at the monthly

459 or yearly scale. However, when considering the total meltwater contribution, the computed fractions for the June-

460 August period agree reasonably well with those recently estimated on a seasonal scale in other high-elevation

461 catchments by Pu et al. (2013) (41 - 62 %, 12 % of glacierized area), Fan et al. (2015) (26 - 69 %), Xing et al. (2015)

462 (almost 60 %) and at the annual scale by Jeelani et al. (2016) (52 %, 3 % of glacierized area), and are even higher than

463 those computed by Mukhopadhyay and Khan (2015) (25 - 36 %). These observations stress the importance of water

464 resources stored within the cryosphere even in catchments with limited extent of glacierized area, such as the Saldur

465 catchment.

466

467 Overall, our tracer-based results on the influence of snowmelt and glacier melt on streamflow agree with glacier mass

468 balance results which revealed important losses from the glacier surface (-428 mm in snow water equivalent) for the

469 year 2012-2013 (Galos, 2013). Particularly, the first strong heat wave serving as melting input was observed in mid-

470 June, when the glacier was still covered by snow and no glacier melt occurred (Galos, 2013), in agreement with our

471 estimates of snowmelt contributions (Fig. 7). Glaciological results also showed that most of the glacier mass loss

472 occurred at the end of July to mid-August 2013, but glacier ablation in the lower part of the glacier (below 3000 m

473 a.s.l.) was observed until the beginning of October (Galos, 2013), corroborating our tracer-based estimates of scenarios

474 A and C (Fig. 7).

475

476 **5.4 Sources of uncertainties in the estimated streamflow components**

477 Various sources of uncertainty affect the estimate of the streamflow components when using mixing models in complex

478 environments such as mountain catchments (Uhlenbrook and Hoeg, 2003; Ohlanders et al., 2013). In cases of mixing

479 model application to separate snowmelt from glacier melt and groundwater, thus not considering rainfall, and in the

480 case of no availability of streamflow measurements (in our case at S8 and S1), uncertainty can be mainly ascribed to the

481 precision of the instrument used for the determination of the tracer signal, and the spatio-temporal patterns of the end-

482 member tracer signature. The instrumental precision can be relatively easily taken into account and quantified by

483 adopting statistically-based procedures (e.g., Genereux et al., 1998). However, the spatio-temporal variation in the

484 hydrochemical signal of the end-members is more challenging to capture and can provide the largest source of

485 uncertainty (Uhlenbrook and Hoeg, 2003; Pu et al., 2013). The isotopic composition and EC of shallow groundwater

12

Hydrology and
Earth System
Sciences
Discussions
Open Access
EGU

486   emerging from springs can be very different within a catchment, especially in cases of heterogeneous geology, as well

487   as the tracer signature of streams at different locations even during baseflow conditions (Jeelani et al., 2010; 2015).

488   The isotopic composition of snowmelt can mainly change according to i) macro-topography (e.g., aspect determines

489   different melting rates and so different isotopic compositions); ii) micro-topography, because small hollows tend to host

490   "older" snow with a more enriched isotopic composition compared to sloping areas; iii) elevation; and iv) season, with

491   δ values becoming more negative with increasing elevation and more positive over the melting season (Uhlenbrook and

492   Hoeg, 2003; Holko et al., 2013; Ohlanders et al., 2013). EC of snow, and therefore, snowmelt can change as well due,

493   for instance, to the ionic pulse at the beginning of the melting season (Williams and Melack, 1991) and/or reflecting

494   seasonal inputs of impurities from the atmosphere (Li et al., 2006), although this variability is usually much more

495   limited compared to that of the isotopes.

496   In our case, the instrumental precision of the isotope analyser and the EC meter is relatively low and was entirely taken

497   into account by the statistical assessment of uncertainty we applied. The spatio-temporal variability of snowmelt was

498   addressed sampling snowmelt at different elevations, aspects and times of the seasons. Finally, we observed a very

499   limited spatial-patterns but a marked seasonal change in the tracer signature of glacier melt (Table 5) that was taken into

500   account in the hydrograph separation application (Table 2). Despite these efforts, logistical issues related to the size of

501   the catchment as well as practical and safety issues related to the accessibility of most areas of the catchment, not only

502   in winter, and, not last, economical issues, prevent a very detailed characterization and quantification of all sources of

503   uncertainty associated to the estimates of the streamflow components at different times of the year and different stream

504   locations. In addition, an underestimation of meltwater fractions due to sampling time not always corresponding to the

505   streamflow peak should be considered (Fig. 8). Specifically, the samples taken on June 19 at S5-USG and S3-LSG were

506   collected almost four hours before the streamflow peak. This means that an additional contribution of snowmelt almost

507   up to 20 % could be expected (Fig. 8). As far as we know, these results have not been reported elsewhere and are

508   critical for a proper assessment of the uncertainty in the estimated component fractions. Moreover, these observations

509   suggest that adequate sampling strategies are critical (Uhlenbrook and Hoeg, 2003) and must be considered when

510   planning field campaigns aiming at the quantification of meltwater in glacierized catchments.

511

512   **5.6 Conceptual model of streamflow components dynamics**

513   The findings from our two previous studies (Penna et al., 2014; Engel et al., 2016) and from the present work allow us

514   to derive a conceptual model of streamflow and tracer response to meltwater dynamics in the Saldur catchment (Fig. 9).

515   To the best of our knowledge, this is the first study to present such a conceptual model of streamflow component

516   dynamics. Although intuitive, this conceptualization is important because represents a paradigm that, given the

517   characteristics of the study site, can be applied to many other glacierized catchments worldwide.

518   During late fall, winter and early spring, precipitation mainly falls in form of snow, streamflow reaches its minimum

519   and is predominantly formed by baseflow. EC in stream water is highest and the isotopic composition is relatively

520   enriched, reflecting the groundwater signal. In mid-spring the melting season begins. The snowpack starts to melt at the

521   lower elevations in the catchment and the snow line progressively moves upwards; stream water EC begins to decrease

522   due to the dilution effect and δ values become more negative, reflecting the first contribution of snowmelt (19 - 39 %).

523   In late spring and early summer the combination of relatively high radiation inputs and still deep snowpack in the

524   middle and upper portion of the catchment provides maximum snowmelt contributions to streamflow (up to 79 ± 6 % in

525   the Saldur River at the highest sampling location) which is characterized by marked diurnal fluctuations and highest

526   melt-induced peaks. Groundwater fractions in stream water become proportionally smaller. The glacier surface is still

527 totally snow-covered, thus glacier melt does not appreciably contribute to streamflow. EC is very low due to the strong
528 dilution effect and the isotopic composition is most depleted. In mid-summer the snowpack is present only at the
529 highest elevations and the glacier surface is mostly snow-free, so that a combined role of snowmelt and glacier melt
530 occurs. Streamflow is characterized by important diurnal fluctuations, but melt-induced peaks tend to be smaller in
531 absolute values than in early summer associated with snowmelt. Although the snowmelt contribution has decreased, EC
532 in the main stream is still very low due to the input of the extremely low EC of glacier melt. On the contrary, the stream
533 water isotopic composition is less depleted compared to late spring and early summer due to the relatively more
534 enriched signal of glacier melt with respect to snowmelt. In late summer snow disappears from most of the catchment
535 and is only limited to residual patches in sheltered locations. The most important inputs to streamflow are provided by
536 glacier melt that reaches its largest contributions (up to 68 - 71 % in the upper monitored Saldur River location).
537 Diurnal fluctuations are still clearly visible but the decreasing radiation energy combined with lower melting supply
538 limits high flows. EC begins to decrease and the isotopic composition to increase. From late spring to late summer low-
539 intensity rainfall events provide limited contributions to streamflow. However, rainfall events of moderate or relatively
540 higher intensity can occur so that rain-induced runoff superimposes the melt-induced runoff and produces the highest
541 observed streamflow peaks. In early fall, meltwater contributions are limited to snowmelt from early snowfalls at high
542 elevations and residual glacier melt and the groundwater proportions become progressively more important. Streamflow
543 decreases significantly and only small diurnal fluctuations are observable during clear days. The two tracers slowly
544 return to their background values.
545
546 **6. Conclusions and future perspectives**
547 Our tracer-based studies (water isotopes and EC) in the Saldur catchment aimed to investigate the water sources
548 variability, the meltwater dynamics and the contribution of snowmelt, glacier melt and groundwater to streamflow in
549 order to contribute to a better comprehension of the hydrology of high-elevation glacierized catchments. We highlighted
550 the highly complex hydrochemical signature of water in the catchment and the main controls on such variability. We
551 applied mixing models to estimate the fractions of meltwater in streamflow over a season, not only at the catchment
552 outlet as usually performed in other studies, but at different locations along the main stream. We found that snowmelt
553 dominated the hydrograph in late spring-early summer, with fractions ranging between 50 ± 5 % and 79 ± 6 % at
554 different stream locations and according to different model scenarios that took into account the spatial and temporal
555 variability of end-member tracer signature. Glacier melt was a remarkable streamflow component in August, with
556 maximum contributions ranging between 8 - 15 % and 68 - 71 % at different stream locations and according to different
557 scenarios. These estimates underline the key role of snowpack and glaciers on streamflow and stress their strategical
558 importance as water resources under changing climatic conditions.
559
560 From a methodological perspective, our results showed that during mixed snowmelt and glacier melt periods, EC and
561 isotopes were not correlated due to the different tracer signature of the two sources of meltwater, whereas they provided
562 a consistent pattern during snowmelt periods only. Such a behaviour, that we found hardly reported elsewhere, should
563 be better assessed over longer time spans and in other sites, but suggests possible simplified monitoring strategies in
564 snow-dominated catchments or during snowmelt periods in glacierized catchments. We identified the main sources of
565 uncertainty in the computed estimates of streamflow component, mainly related to the spatio-temporal variability of the
566 end-member tracer signature, including a clear seasonal enrichment of glacier melt isotopic composition. This is a
567 pattern that must be considered when applying mixing models on a seasonal basis and that we invite to investigate in

568   other glacierized environments. Furthermore, this is the first study, to our knowledge, which quantified the possible

569   underestimation of meltwater fractions in streamflow occurring when stream water is sampled far from the streamflow

570   peak during melt-induced runoff events. Again, this raises awareness about the need of careful planning of tracer-based

571   field campaigns in high-elevation catchments.

572

573   We developed a perceptual model of meltwater dynamics and associated streamflow and tracer response in the Saldur

574   catchment that likely applies to many other glacierized catchments worldwide. However, some limitations intrinsic in

575   our approach should be considered. For instance, the reduced number of rain water samples collected at the rainfall-

576   event scale over the three years did not allow us to fully assess the seasonal role of precipitation on streamflow in

577   relation to meltwater. Furthermore, the use of EC, which integrates all water solutes in a single measurement, cannot

578   differentiate well some water sources and their relation with the underlying geology. Finally, the monthly sampling

579   resolution at different location is useful to obtain a general overview and first estimates of the seasonal variability of

580   streamflow components but high-frequency sampling can certainly help to capture finer hydrological dynamics. In this

581   context, the results of the present work can serve as a very useful basis for modelling applications, particularly to

582   constrain the model parametrization and to reduce the simulation uncertainties, and so to obtain more reliable

583   predictions of streamflow dynamics and meltwater contributions to streamflow in high-elevation catchments.

584

585   **Acknowledgements**

594

595   **References**

596   Aizen, V. B, Aizen, E. M., Melack, J. M, 1996. Precipitation, melt and runoff in the northern Tien Shan. Journal of

597   Hydrology 186: 229–251.

598   Baraer, M., McKenzie, J., Mark, B.G., Gordon, R., Bury, J., Condom, T., Gomez, J., Knox, S., Fortner, S.K., 2015.

599   Contribution of groundwater to the outflow from ungauged glacierized catchments: a multi-site study in the

600   tropical Cordillera Blanca, Peru. Hydrological Processes 29, 2561–2581. doi:10.1002/hyp.10386

601   Barthold, F.K., Tyralla, C., Schneider, K., Vaché, K.B., Frede, H.-G., Breuer, L., 2011. How many tracers do we need

602   for end member mixing analysis (EMMA)? A sensitivity analysis. Water Resources Research 47, W08519.

603   doi:10.1029/2011WR010604

604   Beniston, M., 2012. Impacts of climatic change on water and associated economic activities in the Swiss Alps. Journal

605   of Hydrology 412-413, 291–296. doi:10.1016/j.jhydrol.2010.06.046

606   Blaen, P.J., Hannah, D.M., Brown, L.E., Milner, A.M., 2014. Water source dynamics of high Arctic river basins: water

607   source dynamics of high arctic river basins. Hydrological Processes 28, 3521–3538. doi:10.1002/hyp.9891

Hydrology and
Earth System
Sciences
Discussions

608 Brown, L.E., Hannah, D.M., Milner, A.M., Soulsby, C., Hodson, A.J., Brewer, M.J., 2006. Water source dynamics in a
609   glacierized alpine river basin (Taillon-Gabiétous, French Pyrénées): alpine basin water source dynamics. Water
610   Resources Research 42, W08404, doi:10.1029/2005WR004268

611 Cable, J., Ogle, K., Williams, D., 2011. Contribution of glacier meltwater to streamflow in the Wind River Range,
612   Wyoming, inferred via a Bayesian mixing model applied to isotopic measurements. Hydrological Processes 25,
613   2228–2236. doi:10.1002/hyp.7982

614 Carey, S.K., Quinton, W.L., 2004. Evaluating snowmelt runoff generation in a discontinuous permafrost catchment
615   using stable isotope, hydrochemical and hydrometric data. Nordic hydrology 35, 309–324.

616 Carey, S.K., Quinton, W.L., 2005. Evaluating runoff generation during summer using hydrometric, stable isotope and
617   hydrochemical methods in a discontinuous permafrost alpine catchment. Hydrological Processes 19, 95–114.
618   doi:10.1002/hyp.5764

619 Carturan, L., Zuecco, G., Seppi, R., Zanoner, T., Borga, M., Carton, A., Dalla Fontana, G. Catchment-scale permafrost
620   mapping using spring water characteristics. Permafrost and Periglacial Processes, in press. doi: 10.1002/ppp.1875.

621 Dzikowski, M., Jobard, S., 2012. Mixing law versus discharge and electrical conductivity relationships: application to
622   an alpine proglacial stream: Mixing law versus Q-EC relationships from an Alpine proglacial stream. Hydrological
623   Processes 26, 2724–2732. doi:10.1002/hyp.8366

624 Engel, M., Penna, D., Bertoldi, G., Dell'Agnese, A., Soulsby, C., Comiti, F., 2015. Identifying run-off contributions
625   during melt-induced run-off events in a glacierized alpine catchment: Hydrological Processes, 30: 343–364.
626   doi:10.1002/hyp.10577

627 Engelhardt, M., Schuler, T.V., Andreassen, L.M., 2014. Contribution of snow and glacier melt to discharge for highly
628   glacierised catchments in Norway. Hydrology and Earth System Sciences 18, 511–523. doi:10.5194/hess-18-511-
629   2014

630 Esposito, A., Engel, M., Ciccazzo, S., Daprà, L., Penna, D., Comiti, F., Zerbe, S., Brusetti, L., 2016. Spatial and
631   temporal variability of bacterial communities in high alpine water spring sediments. Research in Microbiology
632   167, 325–333. doi:10.1016/j.resmic.2015.12.006

633 Fan, Y., Chen, Y., Li, X., Li, W., Li, Q., 2015. Characteristics of water isotopes and ice-snowmelt quantification in the
634   Tizinafu River, north Kunlun Mountains, Central Asia. Quaternary International 380-381, 116–122.
635   doi:10.1016/j.quaint.2014.05.020

636 Finger, D., Hugentobler, A., Huss, M., Voinesco, A., Wernli, H., Fischer, D., Weber, E., Jeannin, P.-Y., Kauzlaric, M.,
637   Wirz, A., Vennemann, T., Hüsler, F., Schädler, B., Weingartner, R., 2013. Identification of glacial meltwater
638   runoff in a karstic environment and its implication for present and future water availability. Hydrology and Earth
639   System Sciences 17, 3261–3277. doi:10.5194/hess-17-3261-2013

640 Fischer, B.M.C., Rinderer, M., Schneider, P., Ewen, T., Seibert, J., 2015. Contributing sources to baseflow in pre-alpine
641   headwaters using spatial snapshot sampling: Contributing Sources to Baseflow in Pre-Alpine Headwaters.
642   Hydrological Processes. doi:10.1002/hyp.10529

643 Galos S., 2013. The mass balance of Matscherferner 2012/13. Report of the research project "A physically based regional
644   mass balance approach for the glaciers of Vinschgau – glacier contribution to water availability", funded by the
645   Autonomous Province of Bozen-Bolzano, Italy.

646 Genereux D., 1998. Quantifying uncertainty in tracer-based hydrograph separations. Water Resources Research, 34(4),
647   915–919 .doi:10.1029/98WR00010.

16

Hydrology and
Earth System
Sciences
Open Access
Discussions
EGU

648   Hindshaw, R.S., Tipper, E.T., Reynolds, B.C., Lemarchand, E., Wiederhold, J.G., Magnusson, J., Bernasconi, S.M.,
649   Kretzschmar, R., Bourdon, B., 2011. Hydrological control of stream water chemistry in a glacial catchment
650   (Damma Glacier, Switzerland). Chemical Geology 285, 215–230. doi:10.1016/j.chemgeo.2011.04.012

651   Hoeg, S., Uhlenbrook, S. and Leibundgut, C., 2000. Hydrograph separation in a mountainous catchment - combining
652   hydrochemical and isotopic tracers. Hydrological Processes, 14: 1199–1216. doi: 10.1002/(SICI)1099-
653   1085(200005)14:7<1199::AID-HYP35>3.0.CO;2-K.

654   Holko, L., Danko, M., Dóša, M., Kostka, Z., Šanda, M., Pfister, L., Iffly, J.F., 2013. Spatial and temporal variability of
655   stable water isotopes in snow related hydrological processes. Die Bodenkultur 39, 3–4.

656   Jeelani, G., Bhat, N.A., Shivanna, K., 2010. Use of $\delta^{18}O$ tracer to identify stream and spring origins of a mountainous
657   catchment: A case study from Liddar watershed, Western Himalaya, India. Journal of Hydrology 393, 257–264.
658   doi:10.1016/j.jhydrol.2010.08.021

659   Jeelani, G., Kumar, U.S., Bhat, N.A., Sharma, S., Kumar, B., 2015. Variation of $\delta^{18}O$, δD and 3H in karst springs of
660   south Kashmir, western Himalayas (India). Hydrological Processes 29, 522–530. doi:10.1002/hyp.10162

661   Jeelani, G., Shah, R. A., Jacob, N., Deshpande, R. D., 2016. Estimation of snow and glacier melt contribution to Liddar
662   stream in a mountainous catchment, western Himalaya: an isotopic approach. Isotopes in Environmental and
663   Health Studies. doi: 10.1080/10256016.2016.1186671

664   Jost, G., Moore, R.D., Menounos, B., Wheate, R., 2012. Quantifying the contribution of glacier runoff to streamflow in
665   the upper Columbia River Basin, Canada. Hydrology and Earth System Sciences 16, 849–860. doi:10.5194/hess-
666   16-849-2012

667   Jouzel, J., Souchez, R. A., 1982. Melting-refreezing at the glacier sole and the isotopic composition of the ice. Journal
668   of Glaciology 28(98): 35–42.

669   Kendall, C., McDonnell, J. J., 1998. Isotope tracers in catchment hydrology. Elsevier Science Limiter, Amsterdam.

670   Klaus, J., McDonnell, J.J., 2013. Hydrograph separation using stable isotopes: Review and evaluation. Journal of
671   Hydrology 505, 47–64. doi:10.1016/j.jhydrol.2013.09.006

672   Kong, Y., Pang, Z., 2012. Evaluating the sensitivity of glacier rivers to climate change based on hydrograph separation
673   of discharge. Journal of Hydrology 434-435, 121–129. doi:10.1016/j.jhydrol.2012.02.029

674   Lee, J., Feng, X., Faiia, A.M., Posmentier, E.S., Kirchner, J.W., Osterhuber, R., Taylor, S., 2010. Isotopic evolution of a
675   seasonal snowcover and its melt by isotopic exchange between liquid water and ice. Chemical Geology 270, 126–
676   134. doi:10.1016/j.chemgeo.2009.11.011

677   Li, Zhongqin, Ross, Edwards, Mosley-Thompson, E., Wang, Feiteng, Dong, Zhibao, You, Xiaoni, Li, Huilin, Li, Zhu,
678   Chuanjin, Yuman, 2006. Seasonal variabilities of ionic concentration in surface snow and elution process in snow-
679   firn packs at PGPI Site on Glacier No.1 in Eastern Tianshan, China. Annals of Glaciology, 43A075.

680   Magnusson, J., Kobierska, F., Huxol, S., Hayashi, M., Jonas, T., Kirchner, J.W., 2014. Melt water driven stream and
681   groundwater stage fluctuations on a glacier forefield (Dammagletscher, Switzerland): stream-groundwater
682   interactions on a glacier forefield. Hydrological Processes 28, 823–836. doi:10.1002/hyp.9633

683   Mair E., Leitinger G., Della Chiesa S., Niedrist G., Tappeiner U., Bertoldi G., 2015. A simple method to combine snow
684   height and meteorological observations to estimate winter precipitation at sub-daily resolution. Hydrological
685   Sciences Journal. doi:10.1080/02626667.2015.1081203

686   Mao, L., Dell'Agnese, A., Huincache, C., Penna, D., Engel, M., Niedrist, G., Comiti, F., 2014. Bedload hysteresis in a
687   glacier-fed mountain river: bedload hysteresis in a glacier-fed mountain river. Earth Surface Processes and
688   Landforms 39, 964–976. doi:10.1002/esp.3563

Hydrology and
Earth System
Sciences
Discussions

Open Access
EGU

689 Marshall, S.J., 2014. Meltwater run-off from Haig Glacier, Canadian Rocky Mountains, 2002-2013. Hydrology and
690   Earth System Sciences 18, 5181–5200. doi:10.5194/hess-18-5181-2014
691 Maurya, A.S., Shah, M., Deshpande, R.D., Bhardwaj, R.M., Prasad, A., Gupta, S.K., 2011. Hydrograph separation and
692   precipitation source identification using stable water isotopes and conductivity: River Ganga at Himalayan
693   foothills. Hydrological Processes 25, 1521–1530. doi:10.1002/hyp.7912
694 Mukhopadhyay, B., Khan, A., 2015. A reevaluation of the snowmelt and glacial melt in river flows within Upper Indus
695   Basin and its significance in a changing climate. Journal of Hydrology 527, 119–132.
696   doi:10.1016/j.jhydrol.2015.04.045
697 Mutzner, R., Weijs, S.V., Tarolli, P., Calaf, M., Oldroyd, H.J., Parlange, M.B., 2015. Controls on the diurnal
698   streamflow cycles in two subbasins of an alpine headwater catchment: Diurnal streamflow cycles in an alpine
699   headwater catchment. Water Resources Research 51, 3403–3418. doi:10.1002/2014WR016581
700 Ogunkoya O. O., Jenkins A., 1993. Analysis of storm hydrograph and flow pathways using a three-component
701   hydrograph separation model. Journal of Hydrology 142: 71–88.
702 Ohlanders, N., Rodriguez, M., McPhee, J., 2013. Stable water isotope variation in a Central Andean watershed
703   dominated by glacier and snowmelt. Hydrology and Earth System Sciences 17, 1035–1050. doi:10.5194/hess-17-
704   1035-2013
705 Pellerin B.A., Wollheim W.M., Feng X., Charles J.V, 2008. The application of electrical conductivity as a tracer for
706   hydrograph separation in urban catchments. Hydrological Processes, 22, 1810–1818, doi: 10.1002/hyp.6786.
707 Penna, D., Engel, M., Mao, L., Dell'Agnese, A., Bertoldi, G., Comiti, F., 2014. Tracer-based analysis of spatial and
708   temporal variations of water sources in a glacierized catchment. Hydrology and Earth System Sciences 18, 5271–
709   5288. doi:10.5194/hess-18-5271-2014
710 Penna, D., Stenni, B., Šanda, M., Wrede, S., Bogaard, T.A., Gobbi, A., Borga, M., Fischer, B.M.C., Bonazza, M.,
711   Chárová, Z., 2010. On the reproducibility and repeatability of laser absorption spectroscopy measurements for δ^2H
712   and $\delta^{18}O$ isotopic analysis. Hydrology and Earth System Sciences 14, 1551–1566. doi:10.5194/hess-14-1551-2010
713 Penna, D., Stenni, B., Šanda, M., Wrede, S., Bogaard, T.A., Michelini, M., Fischer, B.M.C., Gobbi, A., Mantese, N.,
714   Zuecco, G., Borga, M., Bonazza, M., Sobotková, M., Čejková, B., Wassenaar, L.I., 2012. Technical Note:
715   Evaluation of between-sample memory effects in the analysis of δ^2H and $\delta^{18}O$ of water samples measured by laser
716   spectroscopes. Hydrology and Earth System Sciences 16, 3925–3933. doi:10.5194/hess-16-3925-2012
717 Penna, D., van Meerveld, H.J., Oliviero, O., Zuecco, G., Assendelft, R.S., Dalla Fontana, G., Borga, M., 2015. Seasonal
718   changes in runoff generation in a small forested mountain catchment: seasonal changes in runoff generation in a
719   forested mountain catchment. Hydrological Processes 29, 2027–2042. doi:10.1002/hyp.10347
720 Pinder G. F., Jones J. F., 1969. Determination of ground-water component of peak discharge from chemistry of total
721   runoff. Water Resources Research, 5(2), 438–445, doi: 10.1029/WR005i002p00438.
722 Prasch, M., Mauser, W., Weber, M., 2013. Quantifying present and future glacier melt-water contribution to runoff in a
723   central Himalayan river basin. The Cryosphere 7, 889–904. doi:10.5194/tc-7-889-2013
724 Pu, T., He, Y., Zhu, G., Zhang, N., Du, J., Wang, C., 2013. Characteristics of water stable isotopes and hydrograph
725   separation in Baishui catchment during the wet season in Mt. Yulong region, south western China. Hydrological
726   Processes 27, 3641–3648. doi:10.1002/hyp.9479
727 Racoviteanu, A.E., Armstrong, R., Williams, M.W., 2013. Evaluation of an ice ablation model to estimate the
728   contribution of melting glacier ice to annual discharge in the Nepal Himalaya: glacial contributions to annual
729   streamflow in Nepal Himalaya. Water Resources Research 49, 5117–5133. doi:10.1002/wrcr.20370

Hydrology and
Earth System
Sciences
Discussions

730 Rock, L., Mayer, B., 2007. Isotope hydrology of the Oldman River basin, southern Alberta, Canada. Hydrological
731   Processes 21, 3301–3315. doi:10.1002/hyp.6545
732 Schaefli, B., Hingray, B., Musy, A., 2007. Climate change and hydropower production in the Swiss Alps: quantification
733   of potential impacts and related modelling uncertainties. Hydrology and Earth System Sciences Discussions 11,
734   1191–1205.
735 Sklash M. G., 1990. Environmental isotope studies of storm and snowmelt runoff generation. In Anderson, M. G., and
736   Burt, T. P., editors: Process studies in hillslope hydrology. Chichester: Wiley, 401-35.
737 Sklash M. G., Farvolden R. N., 1979. Role of groundwater in storm runoff. Journal of Hydrology, 43(1–4), 45–65, doi:
738   10.1016/0022-1694(79)90164-1.
739 Stichler, W., Schotterer, U., Fröhlich, K., Ginot, P., Kull, C., Gäggeler, H., Pouyaud, B., 2001. Influence of sublimation
740   on stable isotope records recovered from high-altitude glaciers in the tropical Andes. Journal of Geophysical
741   Research 106, 22613–22620.
742 Taylor, S., Feng, X., Kirchner, J.W., Osterhuber, R., Klaue, B., Renshaw, C.E., 2001. Isotopic evolution of a seasonal
743   snowpack and its melt. Water Resources Research 37, 759–769.
744 Uhlenbrook, S., Hoeg, S., 2003. Quantifying uncertainties in tracer-based hydrograph separations: a case study for two-,
745   three- and five-component hydrograph separations in a mountainous catchment. Hydrological Processes 17, 431–
746   453. doi:10.1002/hyp.1134
747 Vaughn, B. H., Fountain, A. G., 2005. Stable isotopes and electrical conductivity as keys to understanding water
748   pathways and storage in South Cascade Glacier, Washington, USA. Annals of Glaciology, 40, 1, 107-112, doi:
749   10.3189/172756405781813834
750 Williams, M. W., Melack, J. M., 1991. Solute chemistry of snowmelt and runoff in an Alpine Basin, Sierra Nevada,
751   Water Resour. Res., 27(7), 1575–1588, doi:10.1029/90WR02774.
752 Wohl E., 2010. Mountain rivers revisited, volume 19. ISBN: 978-0-87590-323-1, American Geophysical Union.
753 Xing, B., Liu, Z., Liu, G., Zhang, J., 2015. Determination of runoff components using path analysis and isotopic
754   measurements in a glacier-covered alpine catchment (upper Hailuogou Valley) in southwest China: hydrograph
755   separation; path analysis; glacier-covered catchment. Hydrological Processes 29, 3065–3073.
756   doi:10.1002/hyp.10418
757 Yde, J.C., Knudsen, N.T., Steffensen, J.P., Carrivick, J.L., Hasholt, B., Ingeman-Nielsen, T., Kronborg, C., Larsen,
758   N.K., Mernild, S.H., Oerter, H., Roberts, D.H., Russell, A.J., 2016. Stable oxygen isotope variability in two
759   contrasting glacier river catchments in Greenland. Hydrology and Earth System Sciences 20, 1197–1210.
760   doi:10.5194/hess-20-1197-2016
761 Zhou, S., Wang, Z. and Joswiak, D. R., 2014. From precipitation to runoff: stable isotopic fractionation effect of glacier
762   melting on a catchment scale. Hydrol. Process., 28: 3341–3349. doi: 10.1002/hyp.9911

Tables

Table 1. Sampling years and number of samples collected from the different water sources and used in this study.

Water source	ID of sampling locations	Sampling years	Total n. of samples
Snowmelt	-	2011-2013	24
Glacier melt	-	2012-2013	16
Stream (main river)	S1-S8	2011-2012	535
	S1, S3-LSG, S5-LSG, S8	2013	
Stream (tributaries)	T1	2012	102
	T2, T4, T5	2011-2013	
	T3	2011	
Spring	SPR1-SPR4	2011-2013	84
	SPR6, SPR7	2013	

Table 2. Summary of the properties of the end-members used in the four mixing model scenarios.

Scenario	Groundwater end-member	Snowmelt end-member	Glacier melt end-member
A	Average δ^2H and EC of samples taken from selected springs in fall	Time-invariant isotopic composition and EC	Monthly-variable isotopic composition and EC
B	Average δ^2H and EC of samples taken at each stream location in fall and winter		
C	Average δ^2H and EC of samples taken from selected springs in fall	Monthly-variable isotopic composition and EC	
D	Average δ^2H and EC of samples taken at each stream location in fall and winter		

Table 3. Isotopic composition (δ^2H) and EC of the groundwater end-member used in the two- and three-component mixing model for the four scenarios. n: number of samples; avg.: average; SD: standard deviation.

Sampling day	δ^2H (‰)						EC (µS/cm)					
	Scenarios A and C			Scenarios B and D			Scenarios A and C			Scenarios B and D		
	n	avg.	SD	n	avg.	SD	n	avg.	SD	n	avg.	SD
S1	7	-101.7	5.7	5	-101.5	2.8	5	317.7	76.6	5	257.0	11.4
S3-LSG				3	-101.7	1.4				3	298.0	6.6
S5-USG				4	-101.6	3.0				4	220.4	19.0
S8	5	-98.5	1.3	1	-101.8	(-)0.5*	7	288.2	40.7	1	210.0	(-) 0.1*

*For S8 only one sample was collected during baseflow conditions due to the difficult accessibility of the location in fall and winter. Therefore, no standard deviation could be computed, and the instrumental precision was used for the computation of the uncertainty of the estimated fractions.

Table 4. Isotopic composition (δ^2H) and EC of the snowmelt end-member used in the two- and three-component mixing model for the four scenarios. Abbreviations are used as in Table 2.

| Sampling day | δ^2H (‰)* | | | | EC (µS/cm) | | | | | |
| | Scenarios A and B | | Scenarios C and D | | Scenarios A and B | | | Scenarios C and D | | |
	n	avg.	n	avg.	n	avg.	SD	n	avg.	SD
23 May			1	-195.4				1	15.3	(-) 0.1***
19 June			7	-160.1				7	11.9	22.1
16 July			3	-134.3				3	12.5	14.7
12 Aug.	7	-160.1			13	10.9	17.1			
11 Sept.**			2	-139.9				2	2.9	0.4
18 Oct.**										

*Because the isotopic composition of the high-elevation snowmelt end-member derived by a regression (Eq. 11), the standard deviation was not computed. Thus, the computation of uncertainty was based on the standard error of the estimate of the regression (6.0 ‰) instead of the standard deviation of the samples averaged for each month.

**Because no snowmelt samples were collected in September and October, the August value was used also for the two sampling days in September and October.

***In May 2013, only one snowmelt sample was collected. Therefore, no standard deviation could be computed, and the instrumental precision was used for the computation of the uncertainty of the estimated fractions.

Table 5. Isotopic composition (δ^2H) and EC of the glacier melt end-member used in the three-component mixing model for all scenarios. Abbreviations are used as in Table 2.

| Sampling day | δ^2H (‰) | | | EC (µS/cm) | | |
	n	avg.	SD	n	avg.	SD
16 July	3	-110.7	1.5	3	2.0	0.3
12 Aug.	2	-104.2	3.8	2	2.2	0.7
11 Sept.	2	-92.6	6.5	2	2.5	1.8
18 Oct.*	2	-89.6	4.5	2	2.7	1.7

*No samples were collected on 18 October, when the stream was sampled. Therefore, the tracer value of the glacier melt samples collected on 26 September was used in the mixing model calculations.

Table 6. Basic statistics of isotopic composition (^{2}H) and EC of stream water in the Saldur catchment. CV: coefficient of variation. The other abbreviations are used as in Table 2. Note that for simplicity the negative sign from the coefficient of variation of isotope data was removed.

Period	Statistic	δ²H Saldur River (‰)	δ²H tributaries (‰)	δ²H springs (‰)	EC Saldur River (μS/cm)	EC tributaries (μS/cm)	EC springs (μS/cm)
Entire period (2011-2013)	n	274	102	80	257	102	74
	avg.	-105.3	-103.4	-105.5	166.5	226.8	227.7
	SD	5.2	4.9	6.1	57.1	104.0	77.8
	CV	0.049	0.047	0.058	0.343	0.459	0.342
Summer	n	240	81	68	223	81	62
	avg.	-105.9	-104.5	-107.0	153.7	218.5	229.7
	SD	5.3	4.5	5.1	48.3	100.6	78.3
	CV	0.050	0.043	0.048	0.314	0.460	0.341
Fall-winter	n	34	21	12	34	21	12
	avg.	-101.1	-99.2	-96.9	250.7	258.8	217.2
	SD	2.6	4.0	4.2	32.9	113.0	77.8
	CV	0.026	0.040	0.044	0.131	0.437	0.358

Table 7. Basic statistics of specific discharge, δ²H and EC for the two series reported in Fig. 5. Abbreviations are used as in Table 2.

|	May, June, Sept. 2011-2013				July, August 2011-2013			
	q (m³/s/km²)	δ²H (‰)	EC (μS/cm)	T (°C)	q (m³/s/km²)	δ²H (‰)	EC (μS/cm)	T (°C)
n	12	12	12	12	12	12	12	12
avg.	0.08	-109.3	193.5	5.9	0.15	-107.0	118.3	11.6
SD	0.09	5.2	52.7	5.4	0.04	5.6	25.7	1.0

Figures
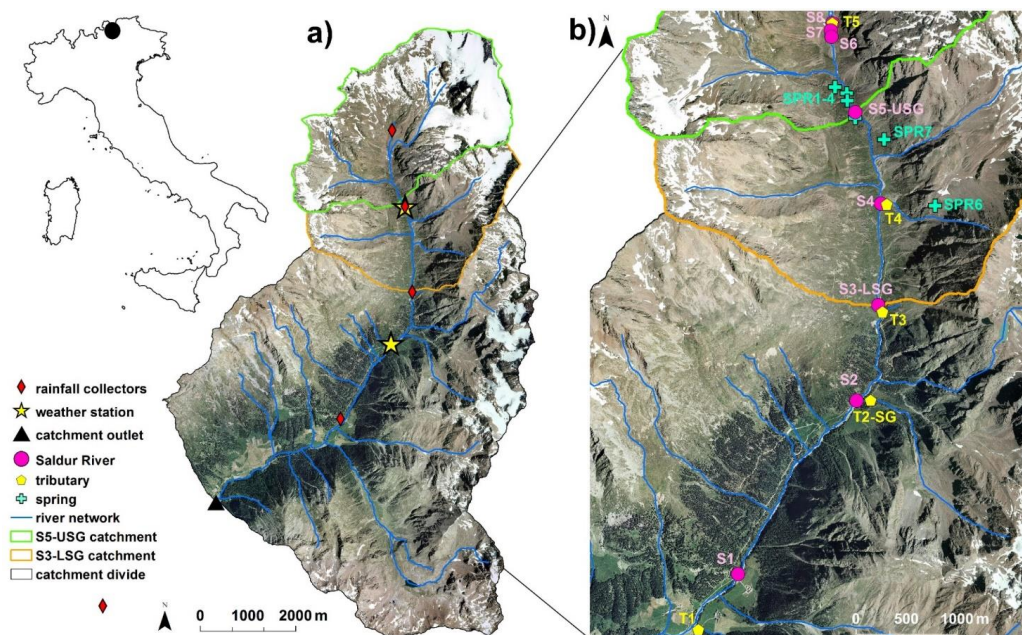
Figure 1. Map of the Saldur catchment, with its localization in the country, and position of field instruments and sampling points. Data from the rainfall collectors were not used in this study but their position is reported for completeness.
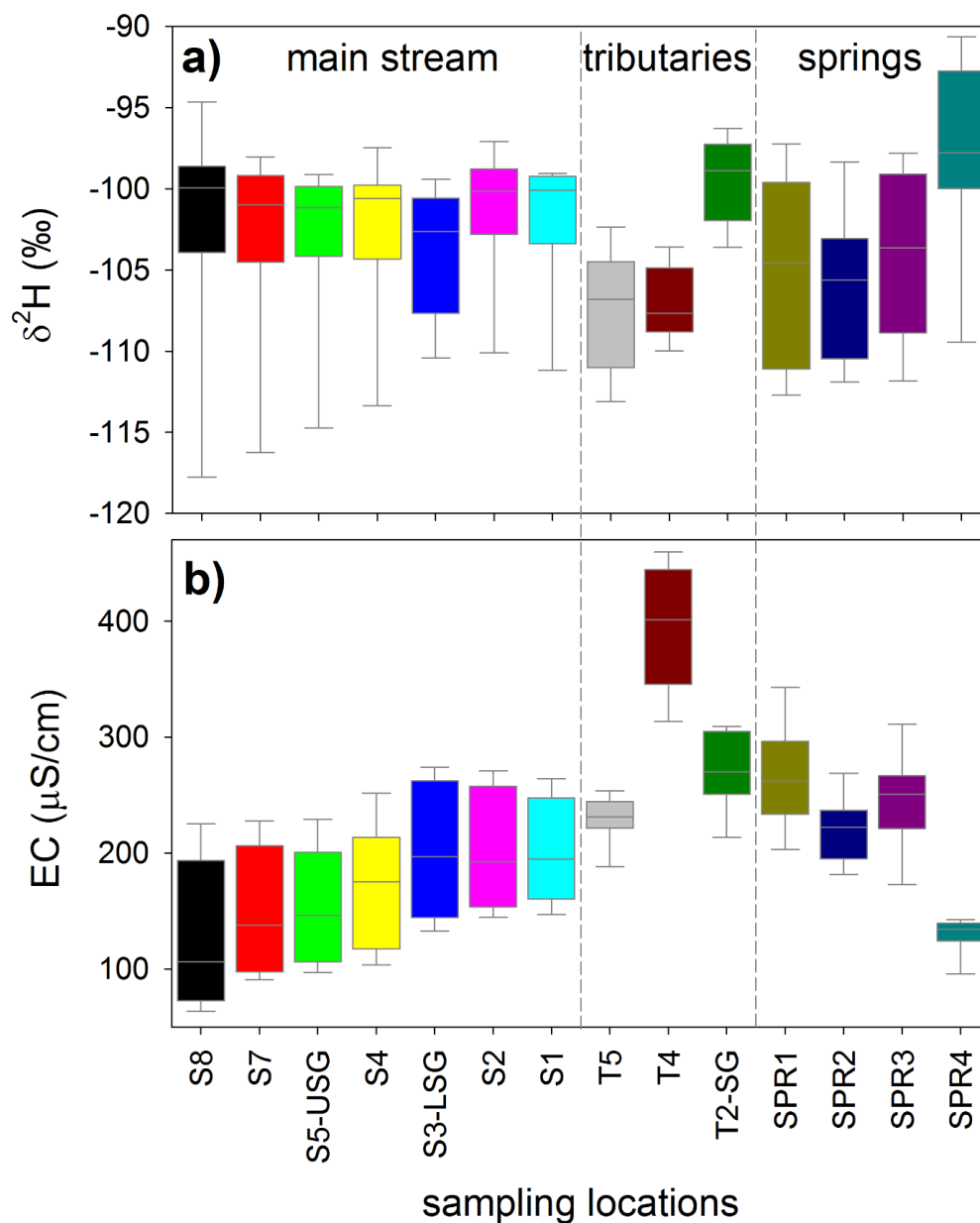
Figure 2. Box-plot of δ²H (panel a)) and EC (panel b)) for samples taken on the same day at all locations in 2011 and 2012 (n = 10 for all locations except for isotope data in T5 and for both tracers at SPR1, for which n = 9). Locations T1 and T3 are excluded because sampled only for one year. The boxes indicate the 25th and 75th percentile, the whiskers indicate the 10th and 90th percentile, the horizontal line within the box defines the median.
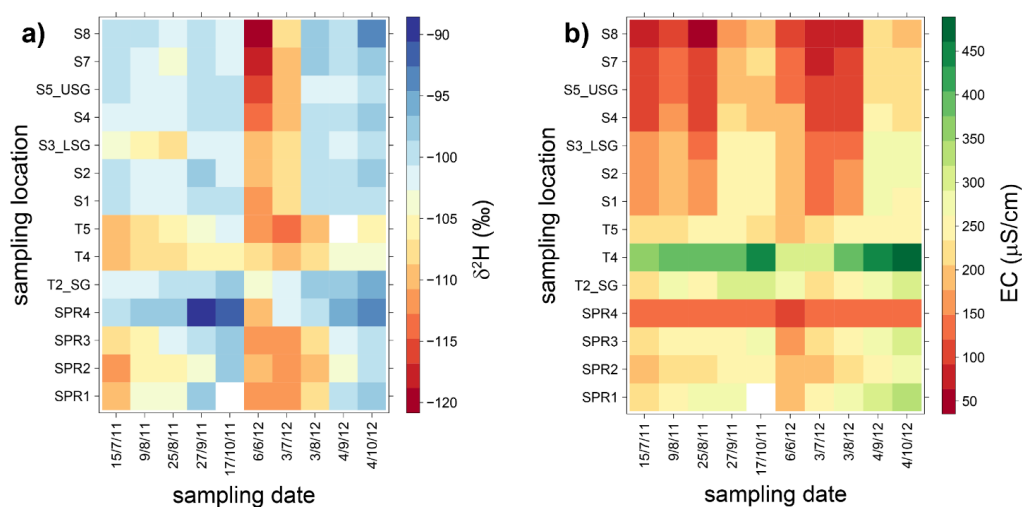
Figure 3. Spatio-temporal patterns of δ^2H (panel a)) and EC (panel b)) for samples taken on the same day at all locations in 2011 and 2012. Location T1 and T3 are excluded because sampled only for one year. White cells indicate no available measurements.
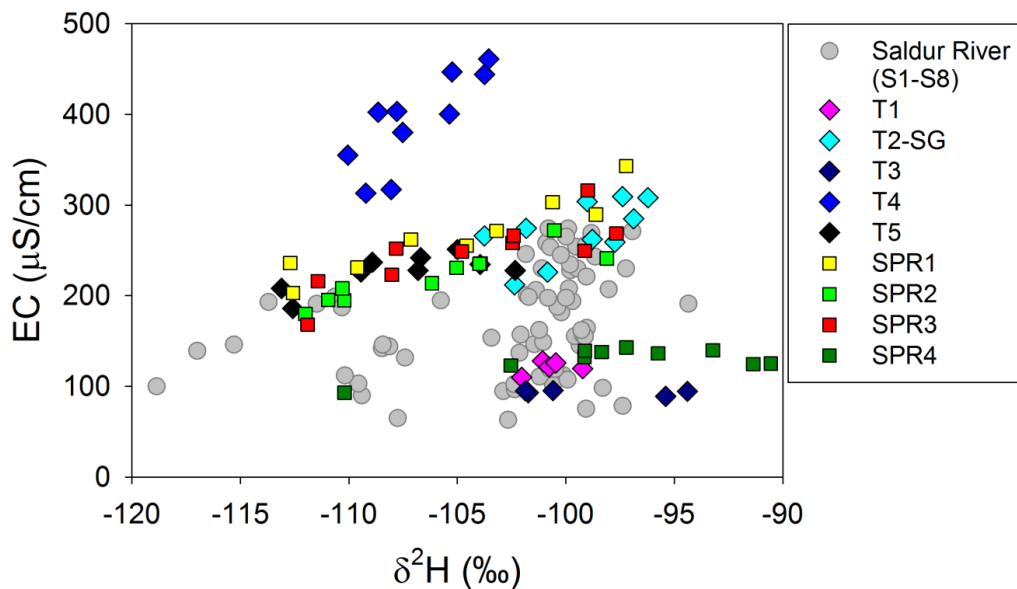
Figure 4. Relation between δ^2H and EC at all locations in the main stream, the tributaries and the springs in 2011 and 2012. Data refer to samples collected at each location on the same days except for T1 and T3, where samples were taken for one year only.
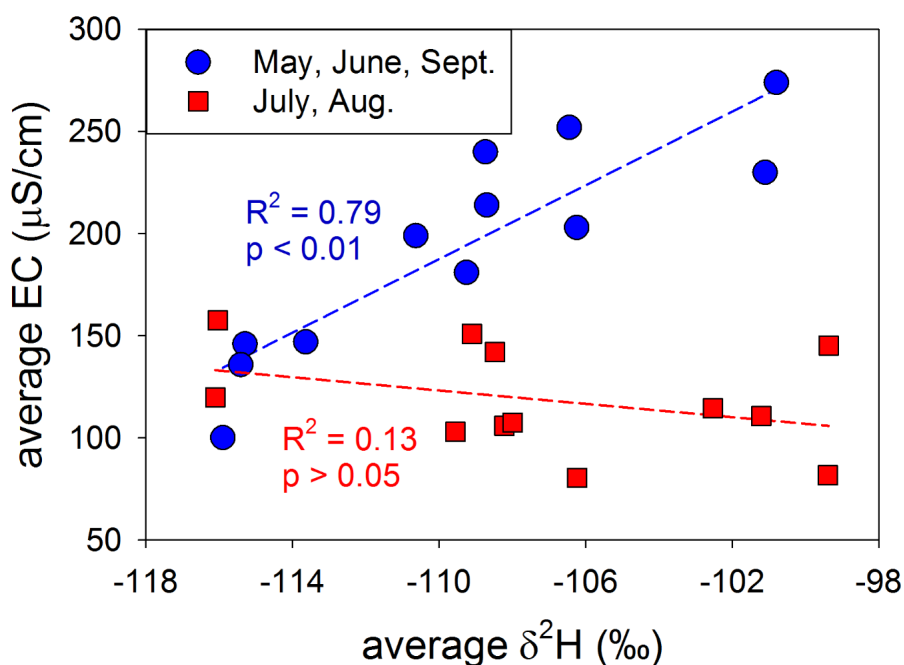
Figure 5. Relation between δ^2H and EC of samples collected at S5-USG and S3-LSG on the same days in 2011, 2012 and 2013, averaged by month.
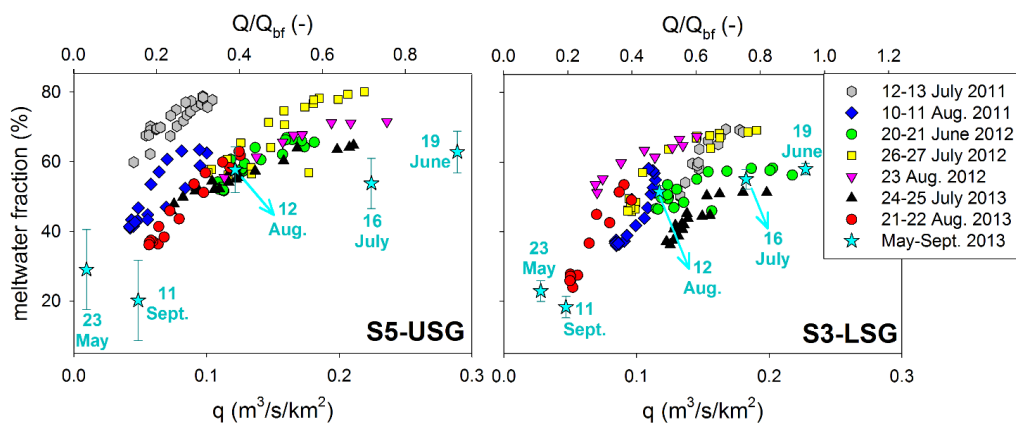


Figure 6. Relation between specific discharge (q) and meltwater fraction (%) in streamflow for the melt-induced runoff events in 2011, 2012 and 2013 sampled at hourly time scale (represented by different coloured symbols), and for the monthly sampling days in 2013 at S5-USG and S3-LSG (represented by stars in cyan). Meltwater fractions for the melt-induced runoff events were taken from Engel et al., (2016), while meltwater fractions for the monthly sampling days in 2013 are given by the average of the four different mixing models scenarios (presented in Fig. 7), and error bars indicate the standard deviation. For the double-peak event on 23-24 August 2012 at S5-USG, where a 9 mm rainstorm superimposed the melt event (c.f. Engel et al., 2016), only the melt-induced part of the event was considered. Discharge is reported also as fraction of the bankfull discharge Q_{bf} at the two sections.

26
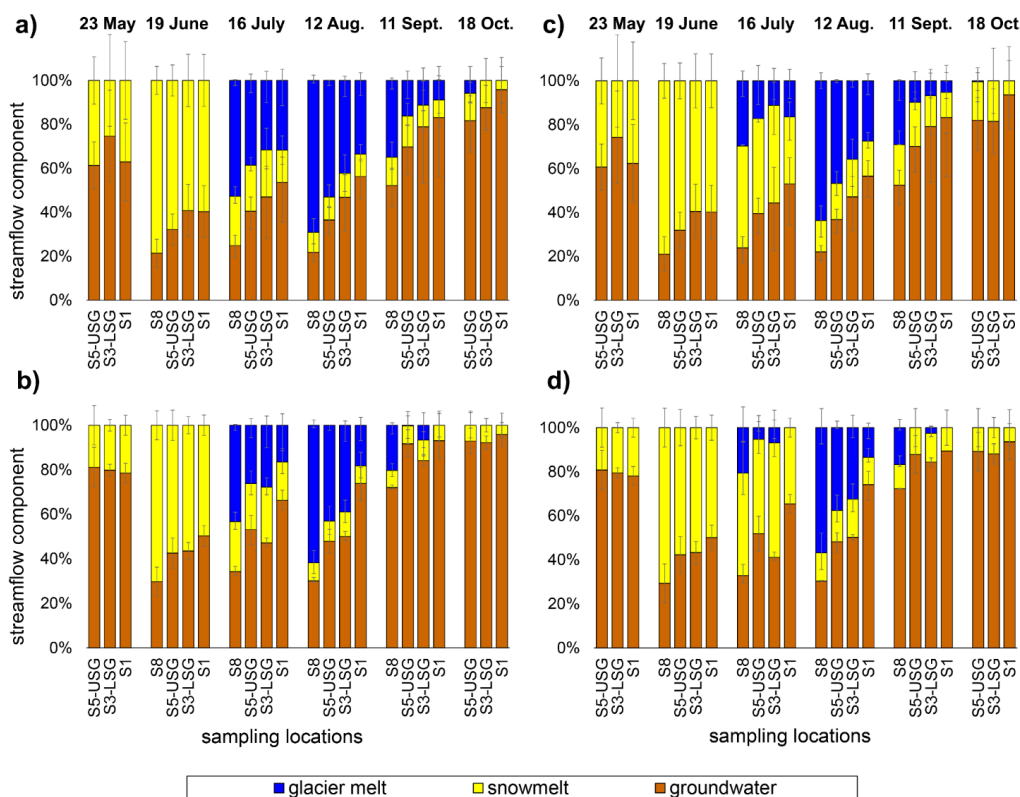
Figure 7. Fractions of groundwater, snowmelt and glacier melt in streamflow for the six sampling days in 2013 at four cross sections along the Saldur River. Left column: the isotopic composition and EC of the snowmelt end-member was considered time invariant, and the groundwater end-member was based on spring data (scenario A, panel a)) or on stream data (scenario B, panel b)). Right column: the isotopic composition of the snowmelt end-member was considered monthly-variable, and the groundwater end-member was based on spring data (scenario C, panel c)) or on stream data (scenario D, panel d)). The error bars represent the statistical uncertainty for each component.

Hydrology and
Earth System
Sciences

Discussions

Open Access

EGU
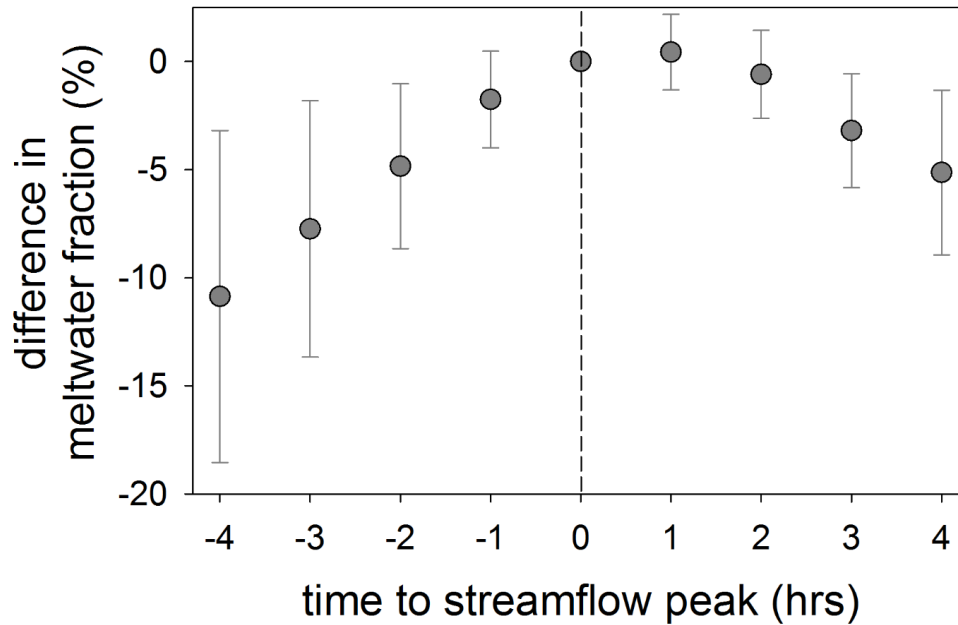
Figure. 8. Average difference between the meltwater fraction in streamflow at the time of streamflow peak and the meltwater fraction at different hours from the time of streamflow peak for the overall 14 melt-induced runoff events at S5-USG and S3-LSG. Error bars represent the standard deviation. The vertical line indicates the time of streamflow peak.

Hydrology and
Earth System
Sciences
Open Access
Discussions
EGU
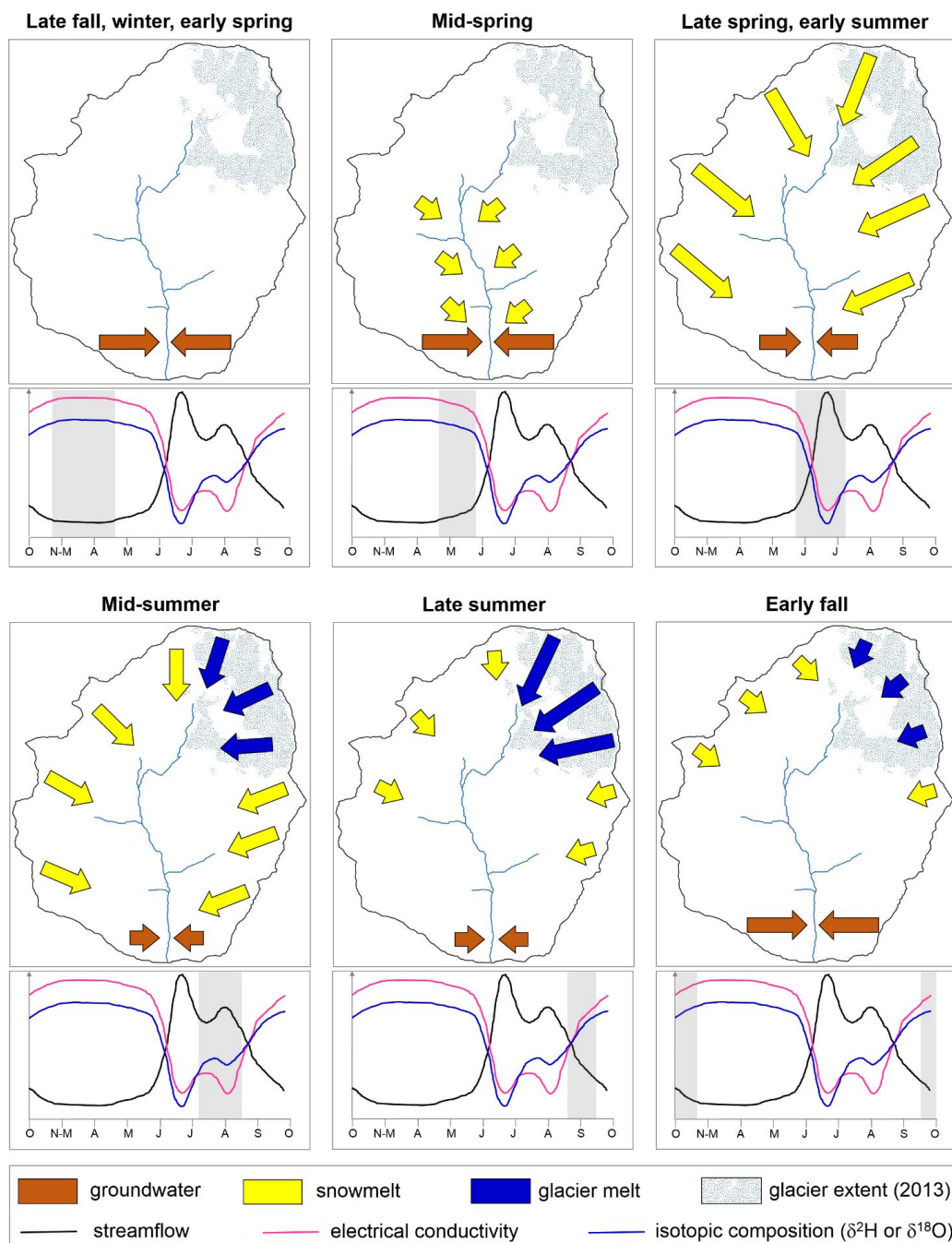
Figure 9. Conceptual model of contributions to streamflow in the Saldur River catchment (closed at LSG). The top subplots in each panel represent the water contributions to streamflow, and the bottom subplots show a sketch hydrograph along with EC and isotopic composition of stream water. The size of the arrows is roughly proportional to the intensity of water fluxes.